

PAPER • OPEN ACCESS

The effect of polyaniline addition on ZnO for the fabrication of high performance photodetection

To cite this article: Dalal K Thbayh *et al* 2020 *IOP Conf. Ser.: Mater. Sci. Eng.* **757** 012074

View the [article online](#) for updates and enhancements.

The effect of polyaniline addition on ZnO for the fabrication of high performance photodetection

Dalal K Thbayh^{1*}, Rawnaq A Talib¹, Kareema M Ziadan²

¹Polymer Research Centre, University of Basra, Iraq

²University of Basra, College of Science, Department of Physics, Basra, Iraq

*Corresponding authors: E-mail address: dalalkarad2014@gmail.com

E-mail address: Rounq4@gmail.com

E-mail address: kmziadan16@gmail.com

Abstract The effect of PANi loading (5 and 15%) on the properties (PANi-ZnO) composite was investigated. X-ray diffraction analysis confirms the hexagonal wurtzite-type ZnO crystal structure, while ZnO peaks' intensity decreases with increasing PANi content. Field emission scanning microscopy observations indicate, in the absence of PANi, ZnO crystallizes as twinned hexagonal rod nanostructure; the size of crystals of ZnO-15%PANi is shorter along ZnO-5% PANi while the width of the crystals is larger with increasing concentration of PANi. The composites deposited onto glass, PET, and Si substrates revealed interesting characteristics for the fabricated photodetector devices. The photodetector based on ZnO-15%PANi / Si substrate demonstrates the best performance with a high gain of 43 and a sensitivity of 4962.

Keywords: ZnO; Polyaniline; Composite; Photodetector; Twin hexagonal.

1. Introduction

Composites of polymer and inorganic material with specific properties are gaining more attention for various applications. There are three main preparations procedures which can be employed to obtain polymer-inorganic composites, namely direct mixing of two or more components in solvent, in situ polymerization of monomer units in the presence of inorganic particles and dissolve mixing of polymer with inorganic particles [1]. The incorporation of inorganic component such as ZnO into polymer matrices could result in the modification of optical, electrical and mechanical properties of the respective components [2]. Polyaniline (PANi) is one of the most studied organic based conducting polymer, with ideal properties for various applications because of its low cost, simple preparation procedure, good environmental stability, and can be easily doped. It is a p-type conducting polymer which can be produced as powder[3], thin film[4], or fiber[5].

Zinc oxide (ZnO) as n-type semiconductor is one of the versatile inorganic compound that can be used in wide range of applications because of its low cost and can be readily produced in various forms such as nanowires [6], nanoflowers [7] nanosheets [8], and nanorods [9].

Ultraviolet (UV) photodetectors based on semiconductor have found applications in water sterilization, human traffic safety, flame sensing, and pollution monitoring systems [10]. Composites and p-n Junction from conducting polymer and metal oxide have been produced for numerous applications such as gas sensors [11], humidity sensors [12], biosensors [13], and photo sensors [14]. However, conducting polymer/ metal oxide composites-based sensors are relatively new and more studies are needed to evaluate the effects of preparation conditions on the evolution of the physical



properties towards the development of high-performance photodetectors. Several researchers have reported on the preparation of ZnO-PAni composite thin films [15-17] and the preparation of twin-structure ZnO with PVP, PEO and PVA [18-20]. More investigation should be conducted on the preparation of twin-structure ZnO with PAni to elucidate its characteristics for sensor applications.

The aim of this research work consists on low temperature growth of twin ZnO - PAni composites. A low cost and simple polymer-ZnO based photodetector is fabricated. The use of glass and silicon as substrates will further reduce the cost of the device. In addition, the use of polyethylene terephthalate (PET) as substrate could provide an advantage due to its flexibility, light weight, transparency, and high resistivity.

2. Experimental and methods

1.0 g zinc acetate hexahydrate ($\text{Zn}(\text{CH}_3\text{COO})_2 \cdot 6\text{H}_2\text{O}$) powder was dissolved in 50 ml of distilled-water then stirred for 10 min at 30°C. After that, 5 ml of (1M) ammonium hydroxide was added to the solution under vigorous stirring at 70°C for 2 h. Subsequently, a certain amount of PAni ($M_w=15,000$ from Sigma-Aldrich) was added to the mixture; 5 and 15 wt.%, then the mixture was kept under stirring for 3h at 50°C. The as-obtained precipitate was washed several times with distilled water to remove any residual reactants and finally dried in oven at 80°C for 1h. The glass substrates, PET, and Si wafer were cut into small square shapes, then cleaned in a beaker containing isopropyl alcohol solution and ethanol alcohol solution in an ultrasonic bath for 15 min. Si substrate was cleaned by Corporation of America (RCA) method [21]. The composites films were deposited onto cleaned substrates by casting technique in formic acid to obtain homogeneous solution.

Morphological observations were performed by field emission scanning electron microscopy (FESEM) using FEI Nova Nano SEM 450. EDX. Structural analysis was checked by high-resolution X-ray diffraction using PANalytical X'Pert Pro MRD system equipped with Cu-K α radiation source ($\lambda=0.1541$ nm). The optical measurements were studied at the room temperature by Raman spectroscopy using JobinYvon HR 800 UV spectrometer. Photoconductivity (UV-sensing) measurements were performed using a current source 2400 source Meter Keithley .

3. Results and discussions

3.1 Morphological observations

Figure 1 illustrates FESEM images of the fabricated powder ZnO / (5,15%) PAni composites. It can be seen obviously the twinning hexagonal rod-type ZnO-PAni composite nanostructures. The crystals in ZnO-15% PAni are shorter than ZnO-5% PAni, while the width is greater at a higher PAni concentration. It is important to highlight that PAni is preferentially adsorbed onto ZnO (0001) face, which will retard the crystal growth perpendicular to this face. Hence, it is suggested that twin-like ZnO has been capped with polymer chain. As it is known that the hexagonal ZnO has the ^+c [0001] direction by zinc-terminated and the ^-c [0001] also direction by oxygen- terminated, so that the positive ion $\text{Zn}(\text{NH}_3)_4^{+2}$ adsorption happens towards ^-c -axis and the negative ion $\text{Zn}(\text{OH})_4^{-2}$ will be adsorbed toward ^+c -axis. After then, the two rods are formed. The as-obtained results are consistent with some previous research works using other kinds of the polymers, such as PVP, PEO-b-PMMA and polyethylenimine (PEI) [18, 19, 22].

The EDX spectrum (Figure 1) reveals the existence of O and Zn elements, in addition to C peaks arising from PAni. It can be seen that the presence of C in ZnO-PAni composite results from an interaction of PAni with ZnO particles. Moreover besides, one can see that the observed percentage of C increases with increasing the weight ratio PAni/ZnO. Hence, it is evident that the addition of PAni has a direct influence on the increase of the diameter of crystal rods in the composites.

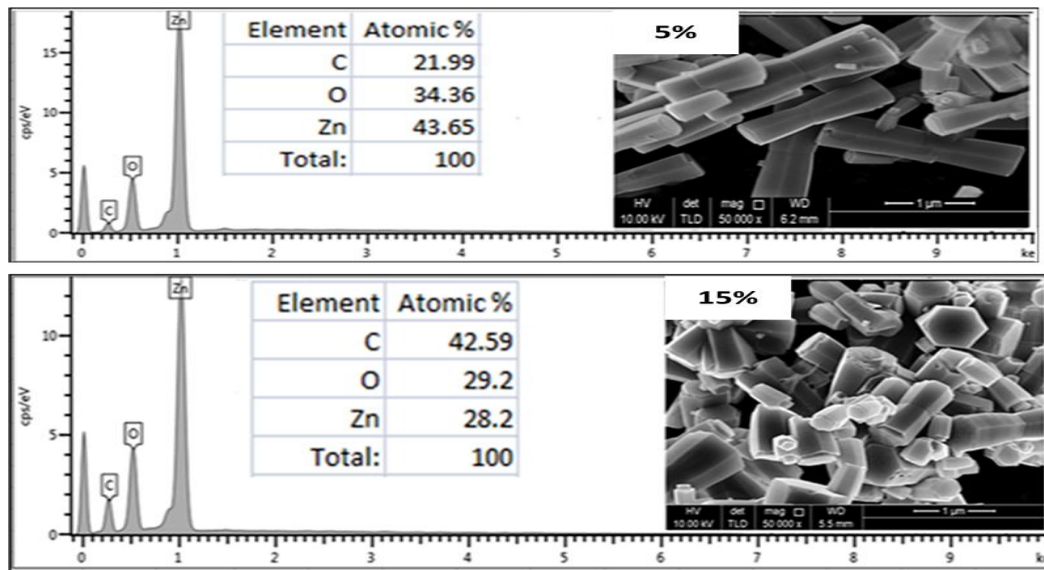


Figure 1. FESEM images and EDX data of (ZnO-5%) PANi, and (ZnO-15%) PANi

Figure 2 shows the surface morphology of the films after dissolving the powder composites in formic acid. It can be noticed that the shape changes from semi-hexagonal large grain distribution (ZnO-5%PANi) to a layered-shaped nanostructure (ZnO-15%PANi). This result indicates that increasing the concentration of PANi in the composite improves its solubility in formic acid, given that the formic acid is a good solvent of polyaniline. Thus, increasing the ratio of PANi to 15 wt% subsequently increases the number of PANi chains between the spaces of ZnO crystalline structure [23], resulting in the formation of a thick composite layer meanwhile semi-hexagonal particles of ZnO-PANI gradually dissipates.

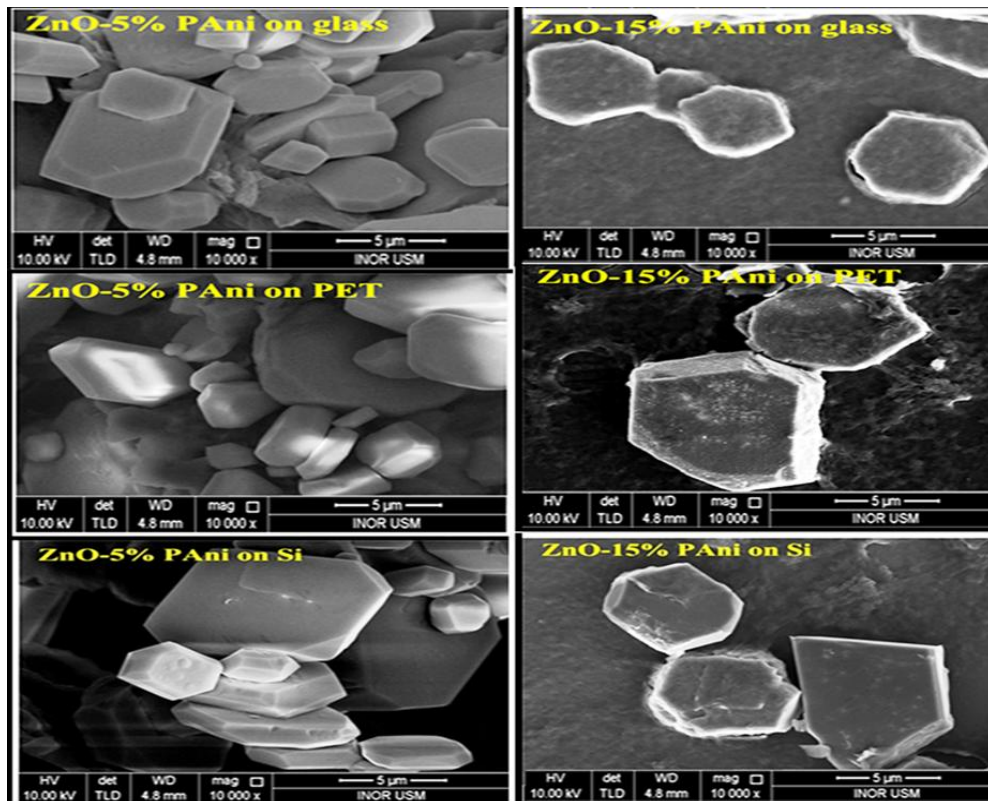


Figure 2: FESEM images of microparticle ZnO-PANI composites deposited on different substrates: glass, PET, and Si.

XRD diffraction patterns of the fabricated ZnO/PANI composites were shown in Figure 3. All that was observed diffraction peaks can be identified within the hexagonal wurtzite-type structure of ZnO phase, in the agreement with JCPDS card No. 80-0075. The minor remaining peak located at $2\theta = 24.42^\circ$ can be assigned to the reflection of PANI. The intense and sharp diffraction peaks indicate the good crystallinity of the as-prepared ZnO-PANI composites. This confirms that the presence of PANi did not modify the original hexagonal structure of ZnO phase without deterring its crystalline quality.

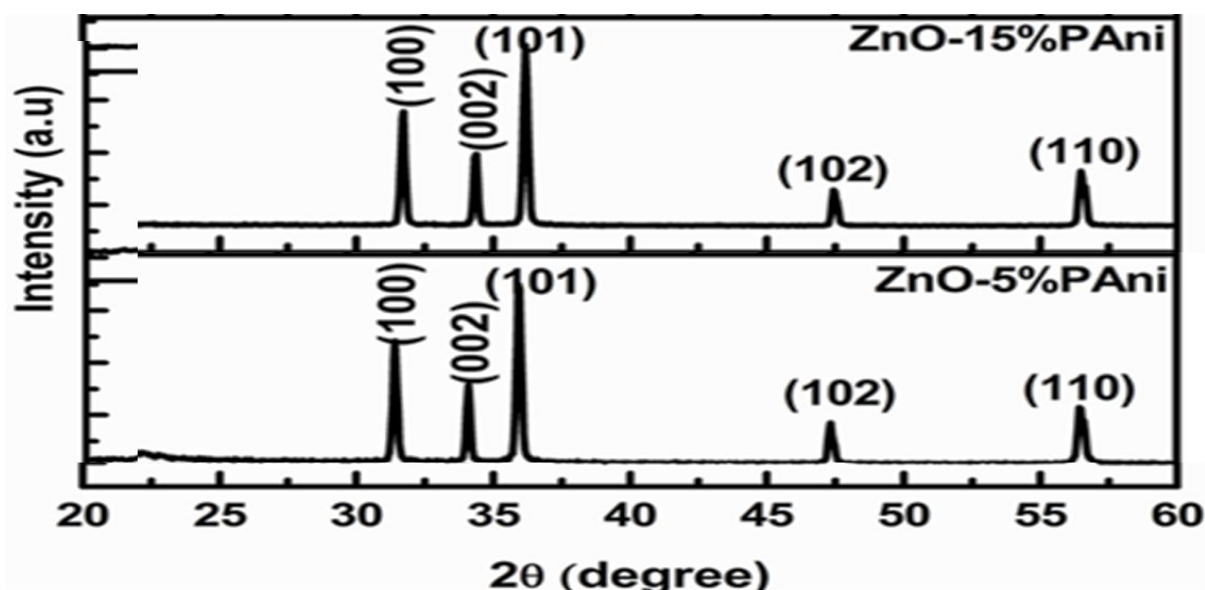


Figure 3: XRD patterns of ZnO-PANI composites at (5-15wt %) ratio of PANi.

The average size of the crystals (G) of ZnO-PANI composites structure has been estimated by measure the full width at half maxima (β) of (101) reflection (Table 1) and using the Debye Scherrer's formula [24, 25]:

$$G = \frac{0.9 \lambda}{B \cos \theta} \quad \dots\dots\dots (1)$$

Where the wavelength(λ) of the X-ray source is equal = 0.15405(nm) , and θ is the angle of the diffraction peak. The crystallite size of ZnO phase increases significantly from 34 nm of (ZnO-5%) PANi to 52 nm of (ZnO-15%) PANi. This might be attributed to a higher surface along the prism plan when compared to the basal plane in the hexagonal close packed crystal structure; thereby more of PANi chain can be expected to become attached to the prism surface of the unit cell rather than that of the basal surface. When the compressive strain is in one direction, there will be a tensile strain on the opposite direction. Thus, the lattice constant is increased along a-axis and caused the unit cell to expand [26-28].

Table 1: Structural properties of ZnO-PANI composites.

Sample	2 θ (degree) (101)	2 θ (degree) (100)	2 θ (degree) (002)	FWHM (degree) (101)	D (nm)	ϵ_z (%)	ϵ_a (%)
ZnO-5% PANI	36.216	31.733	34.333	0.2458	34.00	0.0885	-0.0034
ZnO-15% PANI	36.205	31.730	34.375	0.1604	52.11	-0.0298	0.0057

3.2 Ultraviolet (UV) photodetectors

Figure 4 (a, b and c) displays the repeatability performance of ZnO-PANI composites conducted by applied a varying voltage (1, 3, and 5 V) by using thick film onto glass, PET, and Si

substrates. The device has potential to repeat the same behavior although it has been exposed to the light and dark process over and over. Hence, it could be concluded from that, all the fabricated sensors possess the stability was good during the measurement for 20 sec under 400 nm with an intensity of 0.958 mW/cm^2 , but the sensor based on 15% ZnO-PAni composite onto Si substrate exhibits the best performance. The mechanism of light sensing of ZnO-PAni composites are discussed as follows. Both ZnO and PAni can be excited by light to produce photo-generated carriers and excited electrons, meanwhile the conducting PAni absorbs the light and produces (e^-) that transfers to the CB of ZnO[29]. Simultaneously, the photo-generated holes in VB of ZnO are able to move freely to the composites surface through HOMO PAni.

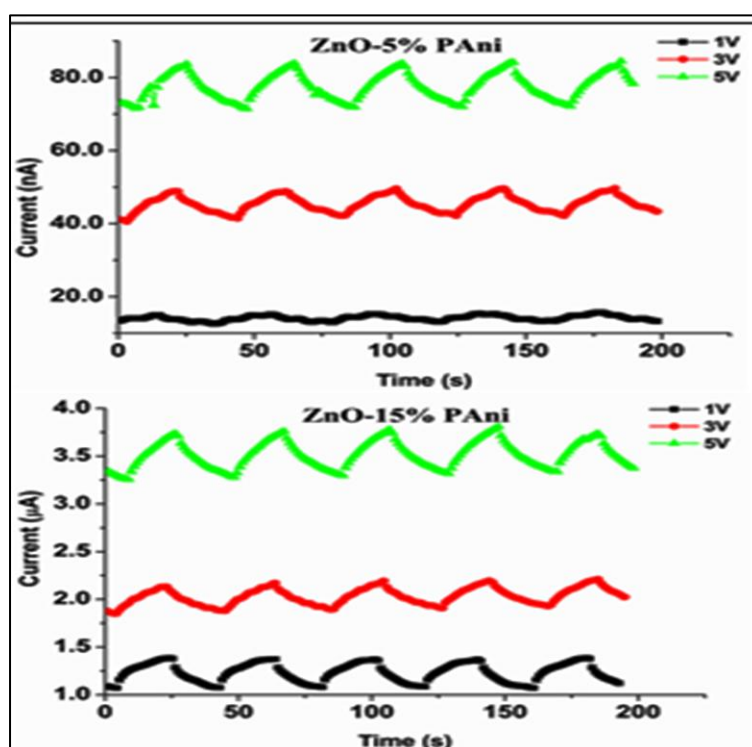


Figure 4: The repeatability characteristic (ON/OFF) of Pt-(ZnO-PAni) composites-Pt on (a) glass substrate under pulsed UV- light (400 nm) at various bias voltages.

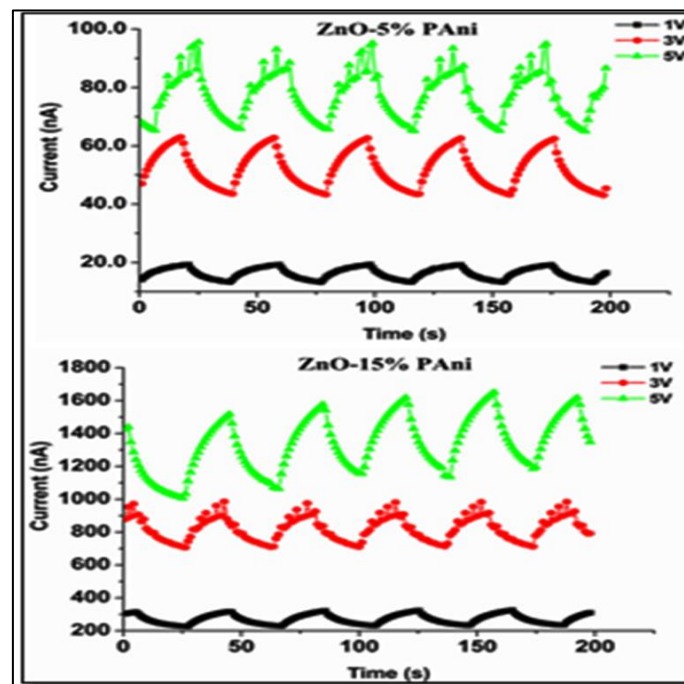


Figure 4: The repeatability characteristic (ON/OFF) of Pt-(ZnO-PANI) composites-Pt on (b) PET substrate under pulsed UV- light (400 nm) at various bias voltages.

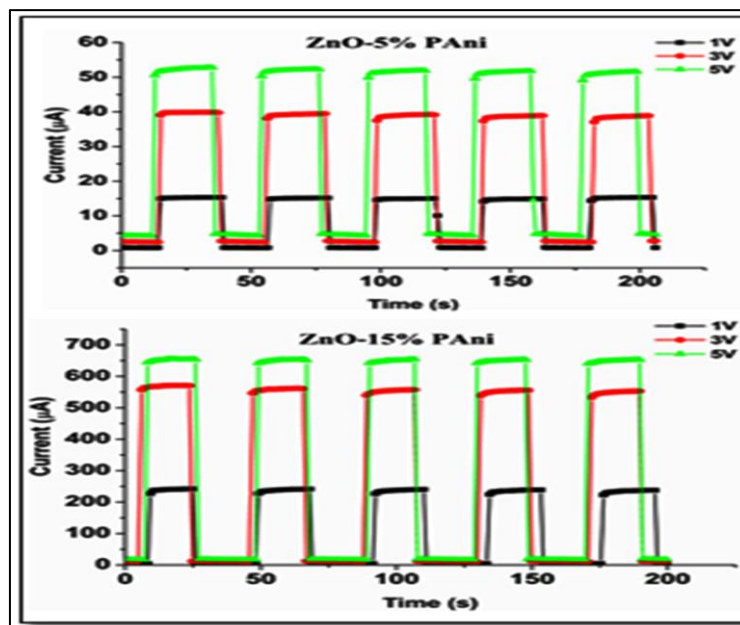


Figure 4: The repeatability characteristic (ON/OFF) of Pt-(ZnO-PANI) composites-Pt on (c) Si substrate under pulsed UV- light (400 nm) at various bias voltages.

So, the photo-generated electrons and holes will move in opposite directions, reducing the recombination probability and making the charge separation more efficient leading to a higher photocurrent [30, 31] as shown in Figure 5. A huge photoconduction sensitivity of the composite deposited onto Si substrate could be due to the higher photon absorption in ZnO-PAni composite layer, whereby some of photo-generated electrons may diffuse to ZnO-PAni/Si junction and subsequently swept into Si side. In general, both layers may contribute to the photocurrent [32], which led to higher sensitivity of ZnO-PAni/Si photodetector as compared to ZnO-PAni composite on insulating substrates (glass and PET). Table 2 summarizes the response time, fall time, sensitivity, and gain measured at various bias voltages for ZnO-PAni composites deposited onto different substrates.

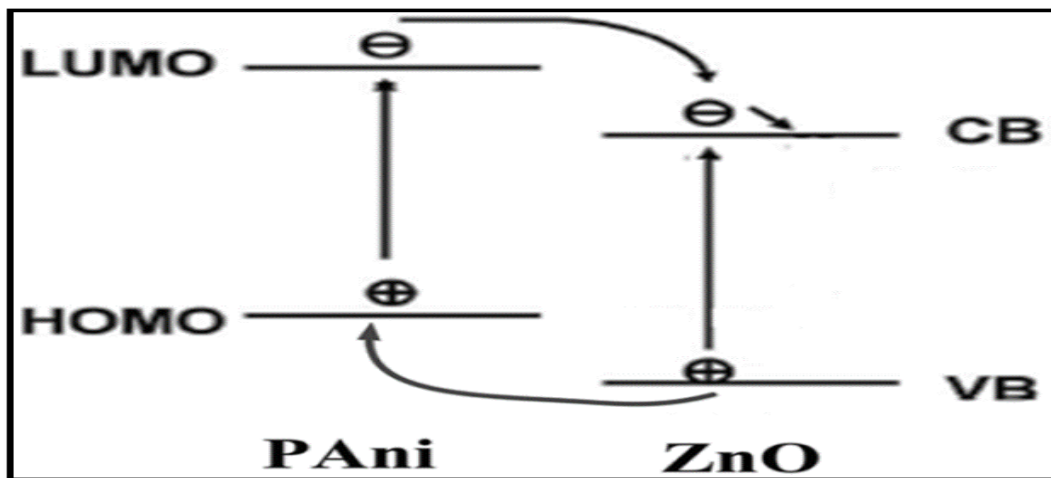


Figure 5: Schematic representation of energy levels and processes involved under UV illumination.

Table 2: The response time, fall time, sensitivity, and gain of the Pt –(ZnO-15%PAni) composites Pt at various bias voltages onto different substrates.

Sample	Substrate	Voltage (V)	Response time (s)	Fall time (s)	Sensitivity %	Gain
ZnO-5%PAni	glass	1	10.93	17.75	15.30	1.18
		3	11.75	15.29	17.39	1.27
		5	13.52	15.98	17.22	1.17
	PET	1	14.64	11.25	43.70	1.45
		3	12.48	14.40	44.30	1.46
		5	8.92	10.82	30.90	1.30
	Si	1	1.052	0.959	2157	25.3
		3	1.067	0.967	1561	16.9
		5	1.072	0.967	991.1	12.3
Sample	Substrate	Voltage (V)	Response time (s)	Fall time (s)	Sensitivity %	Gain
ZnO-15%PAni	glass	1	13.77	11.90	35.30	1.30
		3	15.42	17.40	17.60	1.15
		5	12.68	16.55	16.90	1.13
	PET	1	13.08	13.89	40	1.40
		3	15.69	13.51	28.6	1.31
		5	13.82	14.76	47.1	1.45
	Si	1	0.936	0.852	5925	79.7
		3	1.050	0.956	5450	71.8
		5	0.802	0.885	4962	43

4. Conclusions

ZnO-PAni nanocomposites with enhanced sensing characteristics have been fabricated through cost-effective chemical method starting from the mixture of Zn $(\text{CH}_3\text{COO})_2 \cdot 6\text{H}_2\text{O}$ and PAni. XRD analysis revealed sharp and defined peaks, implying the high crystallinity of the as-prepared ZnO-PAni composites. FESEM observations revealed twinned-hexagonal rod nanostructure; the crystals of ZnO-15%PAni possess smaller length and larger width compared to ZnO-5% PAni,

suggesting that ZnO was capped with polymer. The surface morphology of the as-fabricated composites thick film changed from a nearly hexagonal large grain distribution to a layer shape. The photoconductive properties of the UV thick film deposited onto glass, PET, and Si slides were investigated. The photodetector fabricated from 15% PANi composite onto with Si substrate showed a high gain of 43 and high sensitivity 4962 at voltage of 1 V.

Acknowledgments

The authors would like to thanks Nano Optoelectronics Research and Technology (NOR) of the School of Physics, University Sains Malaysia. Also, they have research support from University of Basrah according to its policy on objectivity in research.

References

- [1] C. S. Wu, Y. J. Huang, T. H. Hsieh, P. T. Huang, B. Z. Hsieh, Y. K. Han, *et al.*, "Studies on the conducting nanocomposite prepared by in situ polymerization of aniline monomers in a neat (aqueous) synthetic mica clay," *Journal of Polymer Science Part A: Polymer Chemistry*, vol. 46, pp. 1800-1809, 2008.
- [2] E. Tang, G. Cheng, X. Pang, X. Ma, and F. Xing, "Synthesis of nano-ZnO/poly (methyl methacrylate) composite microsphere through emulsion polymerization and its UV-shielding property," *Colloid and Polymer Science*, vol. 284, pp. 422-428, 2006.
- [3] L. Ding, X. Wang, and R. Gregory, "Thermal properties of chemically synthesized polyaniline (EB) powder," *Synthetic Metals*, vol. 104, pp. 73-78, 1999.
- [4] N. Agbor, M. Petty, and A. Monkman, "Polyaniline thin films for gas sensing," *Sensors and Actuators B: Chemical*, vol. 28, pp. 173-179, 1995.
- [5] H. L. Wang, R. J. Romero, B. R. Mattes, Y. Zhu, and M. J. Winokur, "Effect of processing conditions on the properties of high molecular weight conductive polyaniline fiber," *Journal of Polymer Science Part B: Polymer Physics*, vol. 38, pp. 194-204, 2000.
- [6] Y. Zhang, M. K. Ram, E. K. Stefanakos, and D. Y. Goswami, "Synthesis, characterization, and applications of ZnO nanowires," *Journal of Nanomaterials*, vol. 2012, p. 20, 2012.
- [7] Z. Wang, X.-f. Qian, J. Yin, and Z.-k. Zhu, "Large-scale fabrication of tower-like, flower-like, and tube-like ZnO arrays by a simple chemical solution route," *Langmuir*, vol. 20, pp. 3441-3448, 2004.
- [8] H. Kou, X. Zhang, Y. Du, W. Ye, S. Lin, and C. Wang, "Electrochemical synthesis of ZnO nanoflowers and nanosheets on porous Si as photoelectric materials," *Applied Surface Science*, vol. 257, pp. 4643-4649, 2011.
- [9] W. I. Park, D. Kim, S.-W. Jung, and G.-C. Yi, "Metalorganic vapor-phase epitaxial growth of vertically well-aligned ZnO nanorods," *Applied Physics Letters*, vol. 80, pp. 4232-4234, 2002.
- [10] J. Sun, F.-J. Liu, H.-Q. Huang, J.-W. Zhao, Z.-F. Hu, X.-Q. Zhang, *et al.*, "Fast response ultraviolet photoconductive detectors based on Ga-doped ZnO films grown by radio-frequency magnetron sputtering," *Applied Surface Science*, vol. 257, pp. 921-924, 2010.
- [11] H. Tai, Y. Jiang, G. Xie, and J. Yu, "Preparation, characterization and comparative NH₃-sensing characteristic studies of PANI/inorganic oxides nanocomposite thin films," *Journal of Materials Science & Technology*, vol. 26, pp. 605-613, 2010.
- [12] P.-G. Su and L.-N. Huang, "Humidity sensors based on TiO₂ nanoparticles/polypyrrole composite thin films," *Sensors and Actuators B: Chemical*, vol. 123, pp. 501-507, 2007.
- [13] A. A. Ansari, G. Sumana, R. Khan, and B. Malhotra, "Polyaniline-cerium oxide nanocomposite for hydrogen peroxide sensor," *Journal of Nanoscience and Nanotechnology*, vol. 9, pp. 4679-4685, 2009.

- [14] G. Paul, A. Bhaumik, A. Patra, and S. Bera, "Enhanced photo-electric response of ZnO/polyaniline layer-by-layer self-assembled films," *Materials Chemistry and Physics*, vol. 106, pp. 360-363, 2007.
- [15] S. P. Ansari and F. Mohammad, "Studies on Nanocomposites of Polyaniline and Zinc Oxide Nanoparticles with Supporting Matrix of Polycarbonate," *ISRN Materials Science*, 2012.
- [16] P. SL, C. MA, and S. Shashwati, "Effect of camphor sulfonic acid doping on structural, morphological, optical and electrical transport properties on polyaniline-ZnO nanocomposites," *Soft Nanoscience Letters*, 2012.
- [17] T. Pandiyarajan, R. Mangalaraja, and B. Karthikeyan, "Enhanced ultraviolet fluorescence in surface modified ZnO nanostructures: Effect of PANI," *Spectrochimica Acta Part A: Molecular and Biomolecular Spectroscopy*, vol. 147, pp. 280-285, 2015.
- [18] M. Öner, J. Norwig, W. H. Meyer, and G. Wegner, "Control of ZnO crystallization by a PEO-b-PMAA diblock copolymer," *Chemistry of materials*, vol. 10, pp. 460-463, 1998.
- [19] T. Thirugnanam, "Effect of polymers (PEG and PVP) on sol-gel synthesis of microsized zinc oxide," *Journal of Nanomaterials*, vol. 2013, p. 43, 2013.
- [20] M. Distaso, M. Mačković, E. Spiecker, and W. Peukert, "Early Stages of Oriented Attachment: Formation of Twin ZnO Nanorods under Microwave Irradiation," *Chemistry-A European Journal*, vol. 18, pp. 13265-13268, 2012.
- [21] A. Uzum, T. Ashikaga, T. Noguchi, H. Kanda, T. Matsuoka, T. Nakanishi, *et al.*, "Water Soluble Aluminum Paste Using Polyvinyl Alcohol for Silicon Solar Cells," *International Journal of Photoenergy*, vol. 2015, 2015.
- [22] X. Hu, Y. Masuda, T. Ohji, and K. Kato, "Polyethylenimine-guided self-twin zinc oxide nanoarray assemblies," *Crystal Growth and Design*, vol. 9, pp. 3598-3602, 2009.
- [23] R. Nosrati, A. Olad, and R. Maramifar, "Degradation of ampicillin antibiotic in aqueous solution by ZnO/polyaniline nanocomposite as photocatalyst under sunlight irradiation," *Environmental Science and Pollution Research*, vol. 19, pp. 2291-2299, 2012.
- [24] P. Prepelita, R. Medianu, B. Sbarcea, F. Garoi, and M. Filipescu, "The influence of using different substrates on the structural and optical characteristics of ZnO thin films," *Applied surface science*, vol. 256, pp. 1807-1811, 2010.
- [25] H. S. Al-Salman and M. Abdullah, "Structural, optical, and electrical properties of Schottky diodes based on undoped and cobalt-doped ZnO nanorods prepared by RF-magnetron sputtering," *Materials Science and Engineering: B*, vol. 178, pp. 1048-1056, 2013.
- [26] S. B. Kondawar, P. T. Patil, and S. P. Agrawal, "Chemical vapour sensing properties of electrospun nanofibers of polyaniline/ZnO nanocomposites," *Advanced Material Letters*, vol. 5, pp. 389-395, 2014.
- [27] D. Sharma, B. Kaith, and J. Rajput, "Single Step In Situ Synthesis and Optical Properties of Polyaniline/ZnO Nanocomposites," *The Scientific World Journal*, vol. 2014, 2014.
- [28] L. Geng, Y. Zhao, X. Huang, S. Wang, S. Zhang, and S. Wu, "Characterization and gas sensitivity study of polyaniline/SnO₂ hybrid material prepared by hydrothermal route," *Sensors and Actuators B: Chemical*, vol. 120, pp. 568-572, 2007.
- [29] S. Ameen, M. S. Akhtar, Y. S. Kim, O.-B. Yang, and H.-S. Shin, "An effective nanocomposite of polyaniline and ZnO: preparation, characterizations, and its photocatalytic activity," *Colloid and Polymer Science*, vol. 289, pp. 415-421, 2011.
- [30] H.-G. Li, G. Wu, M.-M. Shi, L.-G. Yang, H.-Z. Chen, and M. Wang, "ZnO/poly (9, 9-dihexylfluorene) based inorganic/organic hybrid ultraviolet photodetector," *Applied Physics Letters*, vol. 93, p. 153309, 2008.
- [31] L. Wang, D. Zhao, Z. Su, F. Fang, B. Li, Z. Zhang, *et al.*, "High spectrum selectivity organic/inorganic hybrid visible-blind ultraviolet photodetector based on ZnO nanorods," *Organic Electronics*, vol. 11, pp. 1318-1322, 2010.
- [32] M. R. Esmaili-Rad and S. Salahuddin, "High performance molybdenum disulfide amorphous silicon heterojunction photodetector," *Scientific Reports*, vol. 3, 2013.